ResearchGate

See discussions, stats, and author profiles for this publication at: https://www.researchgate.net/publication/7864802

Polymer Patterns in Evaporating Droplets on Dissolving Substrates

ARTICLE *in* LANGMUIR · MAY 2004

Impact Factor: 4.46 · DOI: 10.1021/la0362268 · Source: PubMed

CITATIONS
55

READS
59

2 AUTHORS, INCLUDING:

Ashutosh Sharma IITK

Indian Institute of Technology Kanpur

336 PUBLICATIONS **7,416** CITATIONS

SEE PROFILE

Available from: Ashutosh Sharma IITK
Retrieved on: 01 February 2016

Polymer Patterns in Evaporating Droplets on Dissolving Substrates

Manoj Gonuguntla and Ashutosh Sharma*

Department of Chemical Engineering, Indian Institute of Technology at Kanpur, Kanpur 208016, India

Received November 26, 2003. In Final Form: February 1, 2004

Self-organized polymer patterns resulting from the evaporation of an organic solvent drop on a soluble layer of polymer are investigated. The patterns can be modulated by changing the rate of evaporation and also the rate of substrate dissolution controlled by its solubility. Both of these affect the contact zone motion and its instabilities, leading to spatially variable rates of substrate etching and redeposition that result from a complex interplay of several factors such as Rayleigh−Benard cells, thermocapillary flow, solutal Marangoni flow, flow due to differential evaporation, osmotic-pressure-induced flow, and contact-line pinning−depinning events. The most complex novel pattern, observed at relatively low rates of evaporation, medium solubility, and without macroscopic contact-line stick−slip, consists of a regularly undulating ring made up of a bundle of parallel spaghetti-like threads or striations and radially oriented fingerlike ridges. Increased rate of evaporation obliterates the polymer threads, producing more densely packed fingers and widely separated multiple rings due to a frequent macroscopic pinning−depinning of the contact line. Near-equilibrium conditions such as slow evaporation or increased solubility of the substrate engender a wider and less undulating single ring.

Introduction

When a solution or a particle containing suspension droplet dries, the solute is often distributed on the substrate in interesting ring patterns, usually in the vicinity of a (pinned) contact line. The mesoscopic structures thus produced have been extensively studied due to their potential importance in mesopatterning by organization of particles and other solutes, surface cleaning and coating technologies, preparation of polymer films, optical elements, surface-adhered proteins assays, data storage, microelectronics, and other applications requiring small-scale soft patterns. Since patterns are formed only in the immediate vicinity of the contact line, it is possible to greatly downsize the printed features relative to the size of the solution droplet, leading to novel soft lithography schemes. Some interesting examples of evaporation-assisted patterning are the formation of micron-sized copper lines from a ribbon of copper hexanoate solution,[1] long-range ordering of diblock copolymers by strong droplet pinning,[2] and nanostructuring of conjugate molecules by a stamp-assisted pinning.[3]

Much of the effort has been directed toward patterns formed by evaporation of colloidal particle dispersions. The "coffee-stain problem" studied by Deegan et al.[4−6] reported the formation of ring deposit of particles by drying of a suspension drop. Adachi et al.[7] reported the formation of concentric multiple rings of particles attributed to repeated pinning/depinning of the contact line.

In all of the previous studies, the self-organizing features near a contact line have been studied in evaporating drops of *solutions* (for example, suspensions of metal or latex microspheres, polymer or protein solutions) on *nondissolving* substrates. The objective of this study is to investigate the self-organized patterns that result from the evaporation of an initially pure solvent drop on a *dissolving* substrate. To clearly compare and contrast this study with the earlier works on the drying of solution droplets, we first present some of the known salient features and mechanisms of the patterns in drying solution drops.

The rate of evaporation in a droplet is maximum near the contact line, which causes a flow of liquid and solute toward the contact line,[2,4] often pinning it for some time. The solute concentration thus rises near the contact line. The phenomenon of ringlike stain formation in a dried drop of coffee was explained by this mechanism. Deegan et al.[5] proposed a model to predict the flow velocity, growth rate of the deposited ring, and the distribution of the solute. Formation of distinct multiple concentric rings was also observed in drops containing small particles (0.1 μm), but multiple rings were absent when larger (1 μm) particles were used that prevented depinning.[5] An increase in the localized rate of evaporation near the apex of a droplet yielded a more uniform deposit of solute (rather than a ring pattern) as the redistribution of solute toward the contact line became weaker.[6]

The formation of multiple rings was also reported by Adachi et al.[7] when a suspension droplet was evaporated on a glass slide. In this study, the three-phase contact-line motion seemed to be an oscillatory stick−slip, for which a model was also proposed. The oscillation was suggested to result from the competing friction and surface tension at the contact line. Maeda[8] investigated the concentric ring patterns from evaporating droplets of collagen solutions. The formation of multiple rings and the dynamics of the motion of the contact line were also

* To whom correspondence should be addressed. E-mail: ashutos@iitk.ac.in.

(1) Cuk, T.; Troian, S. M.; Hong, C. M.; Wagner, S. *Appl. Phys. Lett.* **2000**, *77*, 2063.
(2) Kimura, M.; Misner, M. J.; Xu, T.; Kim, S. H.; Russell, T. P. *Langmuir* **2003**, *19*, 9910.
(3) Cavallini, M.; Biscarini, F. *Nano Lett.* **2003**, *3*, 1269.
(4) Deegan, R. D.; Bakajin, O.; Dupont, T. F.; Huber, G.; Nagel, S. R.; Witten, T. A. *Nature (London)* **1997**, *389*, 827.
(5) Deegan, R. D. *Phys. Rev. E* **2000**, *61*, 475.
(6) Deegan, R. D.; Bakajin, O.; Dupont, T. F.; Huber, G.; Nagel, S. R.; Witten, T. A. *Phys. Rev. E* **2000**, *62*, 756.
(7) Adachi, E.; Dimitrov, A. S.; Nagayama, K. *Langmuir* **1995**, *11*, 1057.
(8) Maeda, H. *Langmuir* **1999**, *15*, 8505.

10.1021/la0362268 CCC: $27.50 © 2004 American Chemical Society
Published on Web 03/17/2004

reported by Shmuylovich et al.[9] They quantified the distances traveled between each pinning event and studied the ring formation as a function of particle size and drop radius. A stochastic, rather than a regular stick−slip, motion was however observed, which illustrated that regular pinning/depinning motion is not the only source of radially separated concentric rings. Haw et al.[10] studied the patterns in drying of polymer solutions containing colloidal particles, where formation of several radially oriented convection cells was proposed to explain the undulations of the ring deposit. Nguyen and Stebe[11] studied the patterning of particles by surfactant-enhanced Marangoni instability in evaporating drops of particle suspension. Benard−Marangoni convection-assisted patterning through self-assembly of nanoparticles also occurs in porous zeolite films.[12] Fractal structures and dendritic patterns that form by evaporation of nanoparticle dispersions are controlled by volume fraction of particles and hydrodynamic shear involved in receding motion of the droplet.[13,14] Hydrophilicity or hydrophobicity of the substrate is another important issue influencing the patterns formed. On hydrophilic surfaces, ring patterns are prominently noticed, whereas on hydrophobic surfaces, the particles tend to gather at the center.[15] Warner et al.[16] explained formation of particle "bands" in an evaporating thin film by a hydrodynamic model in which contact lines and trapped pockets of particle containing fluid emerge by a cascading breakup of the film.

Studies on evaporation of a solution (rather than a particle dispersion) have further added to myriad mechanisms responsible for pattern formation.[1,10,12,17−20] For example, confocal microscopy showed that the Marangoni instability of the contact line in evaporating droplets causes waves on its free surface that travel radially inward.[17] On the other hand, concentric rings formed by evaporation of solutions of collagen[18] and polymers[19] have been attributed largely to the formation of multiple Rayleigh−Benard convection cells in the radial direction. Patterning engendered by convection cells was also observed in polymeric films formed by UV-induced polymerization under a vertical temperature gradient.[20]

The only possible general summary of a variety of evaporating drop experiments is that the patterns are formed by a complex interplay of several flows with distinct mechanisms: higher rate of evaporation of liquid near the contact line which induces an advection current in the drop toward the drop periphery; higher solute concentration and lower temperature near the contact line resulting in the solutal Marangoni and thermocapillary flows, respectively; and finally, a gradient of temperature across the dropet in the normal direction due to evaporation at its surface can induce Benard convection in the form of roll cells that grows stronger near the drop periphery due to smaller thickness (higher temperature gradient) there. All of these flows together with possible instability of the contact-line and pinning−depinning events plus substrate−solute (particle) interactions lead to an uneven distribution of the solute and the resulting pattern formation.

Table 1. Vapor Pressures of Solvents and Solubility Parameters of PMMA at 25 °C[a]

solvent	vapor pressure at 25 °C (Pa)	Hildebrand parameter ($\delta_p - \delta_s$)
dichloromethane	5.6×10^4 (HVP)	1.69 (LS)
chloroform	2.57×10^4 (MVP1)	0.09 (MS1)
ethyl acetate	1.24×10^4 (MVP2)	0.0 (HS)
toluene	4.27×10^3 (LVP)	0.16 (MS2)

[a] HVP = high vapor pressure (faster evaporation); MVP1, MVP2 = medium vapor pressure; LVP = low vapor pressure; LS = low solubility; MS1, MS2 = medium solubility; HS = high solubility.

Our aim is to study the patterns formed by a solvent drop evaporating on a dissolving polymeric substrate and the parameters that control these patterns. In such a system, the patterns can be modulated not only by the rate of evaporation but also by changing the rate of dissolution. The key morphological features and their variations with the solvent used (volatility and solubility) and the rate of evaporation are studied. Results for the dissolving polymer substrate are compared and contrasted with the observations when the polymer used is present in the solution drop rather than in the form of the substrate.

Experimental Methods

The model substrate used was a film of PMMA of molecular weight 120K (Aldrich Chemicals), prepared by spin-coating a 6 or 0.1 wt % solution of PMMA in toluene (HPLC grade from E. Merck) onto clean glass slides of size 2.5 cm × 2.5 cm. The glass slides were initially soaked and sonicated in detergent solution for 10 min, then boiled in MEK, acetone, and methanol for 15 min each to remove organic contaminants, and then sonicated again for 5 min in methanol. Finally the slides were rinsed several times in deionized water and dried. With different polymer concentration and different spin speeds, films of about 250 and 20 nm thickness were produced. The film thickness was measured with an ellipsometer and also confirmed with a profilometer (Alpha-step 100, Tencor Instruments, CA). The films were dried at 25 °C for 24 h and in a vacuum at 60 °C for 6 h. They were then stored under vacuum.

A drop of solvent was evaporated on the polymer film thus prepared. The drop volumes varied from 0.5 to 2 μL. The substrate was placed in an enclosed stage with connections for gas flow and sealed with an O-ring. Studies were conducted with different solvents evaporated under ambient conditions and also by varying the rates of evaporation of toluene. The rate of evaporation was reduced by filling the chamber with toluene vapor, and the rate was increased by passing a steady stream of dry nitrogen through the chamber. Experiments were also performed with solvents of different volatility and solubility of PMMA. Different solvents used, their vapor pressure, and solubility parameters of PMMA in the solvents are listed in Table 1. The solubility parameters given are the Hildebrand parameters, where δ_p is the solubility parameter of the polymer (PMMA) and δ_s is that of the solvent. A lower value of ($\delta_p - \delta_s$) indicates higher solubility.

Dichloromethane (high vapor pressure; HVP) is the most volatile among these solvents, and toluene (low vapor pressure; LVP) is the least volatile. The decreasing order of solubility of PMMA in different solvents is ethyl acetate > chloroform > toluene > dichloromethane. All the solvents used were of HPLC grade. The evaporation of drops of polymer solution (PMMA in toluene) on a nondissolving glass substrate was also studied.

The substrate patterns were captured with a CCD camera attached to a Leica DMLM bright field microscope. The motion of contact line was tracked, and the patterns formed at the contact line were recorded. All the experiments were performed at

(9) Shmuylovich, L.; Shen, A. Q.; Stone, H. A. *Langmuir* **2002**, *18*, 3441.
(10) Haw, M. D.; Gillie, M.; Poon, W. C. K. *Langmuir* **2002**, *18*, 1626.
(11) Nguyen, V. X.; Stebe, K. J. *Phys. Rev. Lett.* **2002**, *88*, 164501−1.
(12) Wang, H.; Wang, Z.; Huang, L.; Mitra, A.; Yan, Y. *Langmuir* **2001**, *17*, 2572.
(13) Haidara, H.; Mougin, K.; Schultz, J. *Langmuir* **2001**, *17*, 659.
(14) Mougin, K.; Haidara, H. *Langmuir* **2002**, *18*, 9566.
(15) Uno, K.; Hayashi, K.; Hayashi, T.; Ito, K.; Kitano, H. *Colloid Polym. Sci.* **1998**, *276*, 810.
(16) Warner, M. R. E.; Craster, R. V.; Matar, O. K. *J. Colloid Interface Sci.* **2003**, *267*, 92.
(17) Kavehpour, P.; Ovryn, B.; McKinley, G. H. *Colloids Surf. A* **2002**, *206*, 409.
(18) Maeda, H. *Langmuir* **2000**, *16*, 9977.
(19) Maruyama, N.; Karthaus, O.; Ijiro, K.; Shimomura, M.; Koito, T.; Nishimura, S.; Sawadaishi, T.; Nishi, N.; Tokura, S. *Supramol. Sci.* **1998**, *5*, 331.
(20) Li, M.; Xu, S.; Kumacheva, E. *Langmuir* **2000**, *16*, 7275.

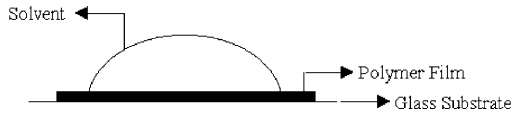

Figure 1. Schematic of an evaporating drop on a dissolving thin film of polymer substrate.

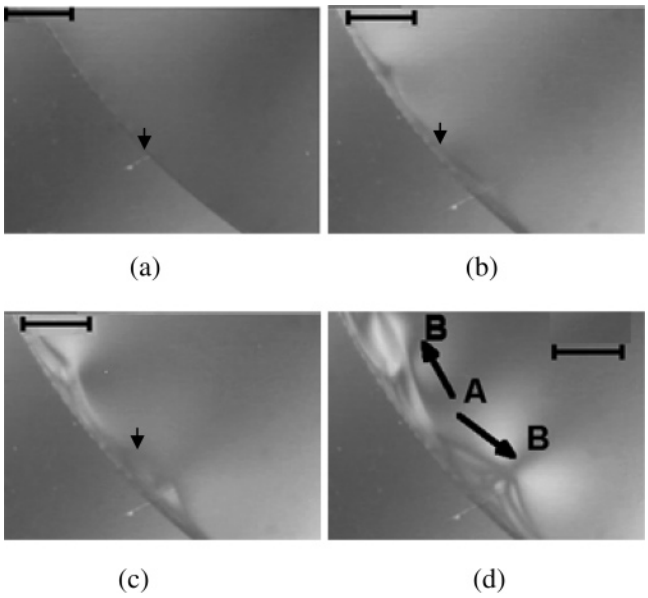

Figure 2. Development of polymer periodic patterns near the contact line in an evaporating toluene drop in ambient: (a) 3, (b) 10, (c) 20, and (d) 40 s. The short arrows indicate the position of the contact line. The bar in the images is 200 μm. The substrate is a 200 nm thick PMMA layer in all the figures, except in Figure 13. In picture d, long arrows depict the flow along the contact line from polymer-depleted regions A (thinner) to polymer-rich regions B (thicker).

ambient temperature of 25 °C. Repeating the experiments on different days checked the repeatability of the experiments.

Results and Discussion

We first report the general features of the pattern formed after the drop is completely evaporated and then correlate them with the dynamics of contact line motion, rate of evaporation, and solubility. A schematic of the system is shown in Figure 1. The drop initially spreads rapidly on the substrate and attains a quasi-equilibrium contact angle. The solute concentration in the drop increases with time due to the substrate dissolution. The evaporation results in a continuous decrease of the drop volume thereafter and further increases the solute concentration.

Figures 2 and 3 show the dynamics of contact line and the "wet" polymer patterns formed when a toluene drop of initial volume 1 μL dewets the surface under ambient conditions. The short arrows indicate the position of the contact line. The contact zone during the droplet evaporation presented a crumpled appearance, indicating periodically arranged thicker and thinner regions of the polymer solution near the contact line (Figure 13 shown later gives an even better view of the receding contact zone). The long arrows indicate the direction of local flow along the drop periphery from the thinner to thicker regions (A → B) as could be clearly visualized under a microscope. It is interesting to note also that the solvent first retracts from the thinner regions A, followed by the thicker regions B. This indicates that polymer fingerlike patterns are formed by polymer deposition from the solution, rather than by a differential etching of the polymeric substrate.

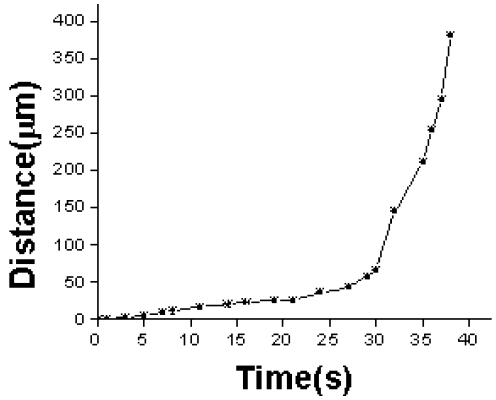

Figure 3. Distance traveled by the contact line of toluene drop from the edge during evaporation in ambient. The vertical axis is the distance measured from the edge of the drop. Note the absence of macroscopic stick−slip motion of the contact line.

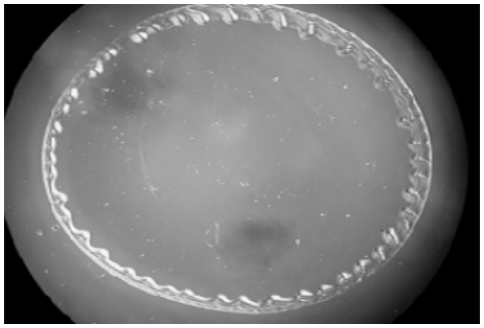

Figure 4. Micrograph of the ring formed after complete evaporation of toluene in ambient air at 25 °C (medium rate of evaporation). There is absence of features or multiple rings beyond the initial ring. The initial drop diameter was 3 mm.

The thickness of the solvent film at the edge of the drop is thin, and the solvent evaporates and recedes quickly (<35 s) there, freezing the polymer pattern near the initial contact line. There are two kinematically distinct regimes of edge retraction: a slow (35 s) phase followed by a fast shorter phase of about 15 s duration. There is no clear indication of a macroscopic stick−slip in the either phase. The time taken for complete evaporation of the drop was quite reproducible to about 50 ± 2 s. In the initial slow phase (Figure 2A−C), rudiments of an undulating wet polymer structure develop along the contact line, which rapidly grows into the final structure (Figure 2D) from which the contact line detaches and recedes quickly in the fast phase. No further features such as multiple rings are formed away from the initial location of the contact line (Figure 4). The full development of the structure with well-defined morphology, periodicity, and significant radial orientation (Figure 2D) occurs within a narrow window of time (25−35 s). Figure 4 shows a coarse droplet scale view of the final pattern, and Figure 5 shows the finer details of the pattern formed along the initial edge of the drop after complete evaporation of the solvent. Images A−E of Figure 5 are sampled at different locations along the rim and summarize all the different general shapes witnessed. Structures in figures A, B, and C lack a very prominent radial orientation in the form of narrow fingerlike projections that are more developed in patterns D, E, and F. The more pronounced radially oriented features developed where the contact line receded faster. In all of the patterns (A to E), two distinct types of structures, oriented azimuthally and radially, are visible in varying proportions. The first is a ring of deposits that undulates rather periodically both in its thickness and its

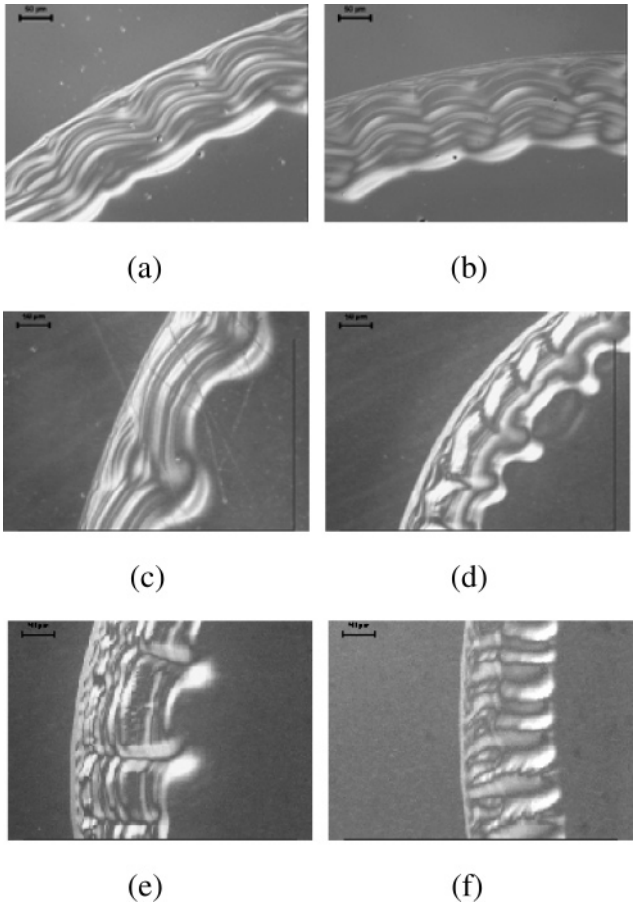

Figure 5. Patterns formed after evaporation of a toluene drop in the ambient (medium rate of evaporation). The periodic undulations (ridges and valleys) and the spaghetti features form along the drop periphery. The scale bars in all figures correspond to 50 μm.

width. The outside edge of the pattern does not exhibit undulations, but the inner part of the ring shows rather evenly spaced broad fingers along the periphery (Figure 4). Second, the regularly undulating ring often consists of a complex pattern of a bundle of spaghetti-like threads (striations) oriented along the contact line (azimuthally). The bundle undulates rather regularly in height to form radially oriented ridges (fingers) and intervening valleys. The prominence and abundance of spaghetti-like threads and ridges vis-à-vis the radially oriented fingers vary along the periphery.

What are the mechanisms leading to the most general type of structure along the periphery of an evaporating solution drop? Figure 6a−d gives schematic sketches of various flows that cooperate to produce radial and azimuthal variations of the polymer concentration along the slowly receding (or pinned) contact line. To begin with, a lower thickness and possibly a higher rate of evaporation of the solvent near the contact line increases the polymer concentration by dissolution there as compared to the droplet center. Also, if polymer diffusion and convective mixing across the height of the drop are small, concentration can be significantly higher at the polymer−solvent interface, at least in the initial stages of evaporation. Thus, the thin contact zone should be nearly saturated ahead of the central regions. Further polymer is brought to the drop periphery from the central regions by at least four distinct mechanisms: (1) If the contact line does not move enough to compensate the evaporative loss (the extreme case being pinning of contact-line) or evaporation near the contact line is higher, mass balance dictates a radial

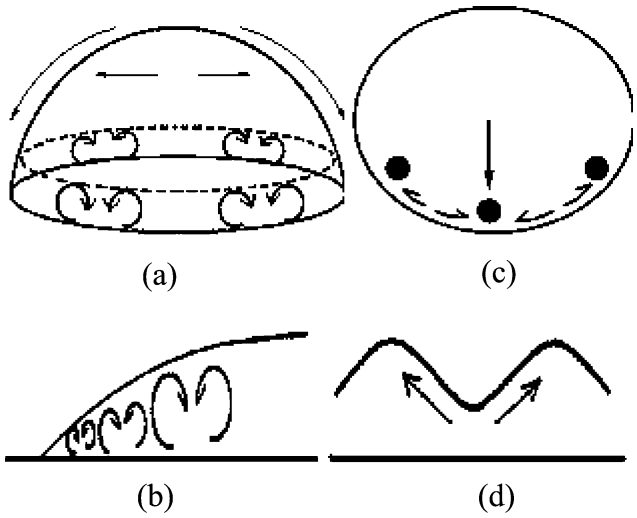

Figure 6. Schematic of the flows that occur during evaporation of the solvent on a dissolving substrate. (a, b) The formation of Benard convection cells near the contact line in a thin contact zone due to a strong thermal gradients normal to the substrate caused by evaporative cooling. (a) and (b) show the multiple cells along the drop periphery and in the radial direction, respectively. (c) is a cartoon where the dark spots indicate the position of thicker contact zone with higher local polymer concentration and convection from the thinner to thicker regions (toward the polymer rich regions). (d) is a schematic of the same local flows along the periphery from the thinner to thicker regions caused by solutal Marangoni, thermocapillarity, and osmotic pressure differences. The flow from the thinner to thicker regions along the drop periphery, leading to a spatially periodic deposition of polymer, was clearly discerned during the evaporation (Figures 2 and 13).

flow toward the periphery to replenish the evaporative losses. This is the classical mechanism usually invoked for the "coffee-stain" problem. (2) A thermocapillary flow occurs toward the periphery if surface temperature there is lower (surface tension is higher) due to faster evaporative cooling. (3) Since surface tension is expected to increase with increased polymer concentration (polymer has higher surface tension than the solvent), a solutal Marangoni flow toward the periphery should also occur due to increased polymer concentration there. (4) Higher concentration of polymer in a good solvent also implies a higher osmotic pressure that can cause flow from the dilute central regions toward the periphery. The last two mechanisms seem not to have been discussed previously in this context. The net result of all these outward radial flows is an enhancement of polymer concentration near the contact line, which in any case is increasing due to evaporation and substrate dissolution. The polymer should begin to get redeposited when its concentration exceeds a critical supersaturation and stop when it drops below its saturation level. The cycle of polymer etching, replenishment, deposition, and depletion can continue if the contact-line movement is slow until the polymer, present as the soluble substrate, is exhausted. This could explain the formation of successive polymer threads (spaghetti features in Figure 5) in the initial slow retraction regime. An alternative explanation of these features would have to invoke repeated and rapid pinning and depinning (stick−slip) of the contact line,[6] which is not in conformity with the contact-line dynamics of Figure 3. The point is that the formation of closely spaced parallel polymer threads can occur even in a sufficiently slowly moving contact line by the same mechanisms that engender the well-studied, widely separated concentric solute rings by macroscopic stick−slip motions of the contact line. This

indicates new possibilities for the control of finer and more densely packed polymer structures by tuning the kinetics of contact-line motion vis-à-vis the mechanisms of polymer enrichment and depletion near the contact line (for example, solubility and rates of evaporation and substrate solubilization). Indeed, as we show below, the stratified structure of polymer threads in Figure 5 can be suppressed at both low and high rates of evaporation, by changing the solvent, by depletion of the substrate polymer film and also in the case of the evaporation of the polymer solution, rather than evaporation on a dissolving substrate. These observations, especially the last one, seem to suggest a crucial role for a finely balanced competition between the kinetics of dissolution and rate of evaporation for the formation of a stratified ring. Thus, although in some systems multiple Benard cells[1,9,11] in the radial direction (Figure 6b) may result in the multiline structures from evaporating *solution* drops, this explanation is less likely for our case, where stratified structures were absent in the solution drops with a wide range of initial polymer concentration (0.1−1 wt %).

We now turn to the possible mechanisms for the formation of fairly periodic, radially oriented fingerlike features or the ridge and valley structures shown in Figures 4 and 5. The regularly spaced ridges (fingers) and intervening valleys indicate a periodic nonuniform deposition of polymer along the contact line. The contact zone rapidly transforms during the initial evaporation into periodically arranged thicker (polymer rich) and thinner (polymer depleted) regions as seen in Figure 2 (and later in Figure 13). The thick polymer deposits (hills or fingers) form after complete evaporation of solvent from the thicker regions. The flow from the thinner to the thicker regions (A → B in Figures 2 and 13) was clearly discernible under the microscope during evaporation. This flow is shown schematically in Figure 6c,d. The periodic variations of contact-zone thickness and polymer concentration can also be understood in terms of the four basic flows discussed above, namely, the formation of multiple Benard convection cells *along the contact line* (Figure 6a), thermocapillarity, solutal Marangoni flow, and osmotic-pressure-driven flow. The last two are driven by the concentration nonuniformity, from the polymer-depleted to the polymer-rich regions (Figure 6c,d). Thermocapillarity would also aid destabilization if valleys have higher temperature than the hills by virtue of evaporatively cooled surface of the thin regions being closer to the more nearly isothermal substrate. Finally, the Benard cells (along the contact line) could also form because the temperature *gradient across* the *thin* solvent film close to the contact line is large. The convection cells can be formed only if the temperature gradient across the layer exceeds a critical value,[1] which would explain their presence near the *periphery* of the evaporating drop in a thin contact zone. Figure 6a shows a schematic of the convection cells that would enrich the polymer toward their centers. In addition, it may also lead to a bulging of the free surface near the cell center. On the scale of a single convection cell, an increased polymer concentration at its center attracts additional flows due to the solutal Marangoni effect and osmotic pressure imbalance. Both of these flows are directed from the lower to higher concentration regions (Figure 6c,d), thus further enhancing the polymer concentration and favoring a spatially periodic redeposition at the center of convection cells, resulting in the formation of periodic ridges and valleys along the contact line. As shown below, a faster rate of evaporation accompanied by a more rapid contact line movement diminishes the spaghetti-like features but makes the radially oriented fingers more

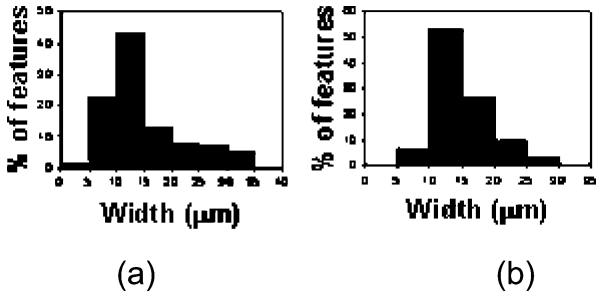

Figure 7. Distribution of the width of the spaghetti features: (a) toluene, case LVP; (b) ethyl acetate, case MVP2.

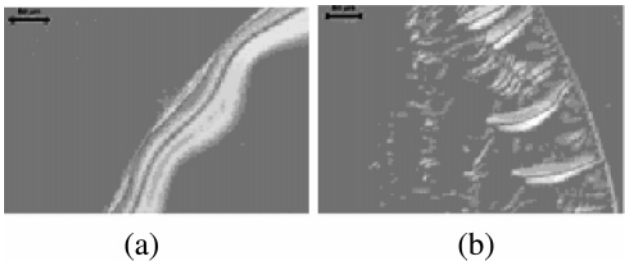

Figure 8. Features formed on varying the rate of evaporation. (a) Low rate of evaporation of toluene in surrounding atmosphere filled with toluene vapors leads to a single thick and wide ring with increased periodicity along the periphery. (b) High rate of evaporation in a steady stream of dry nitrogen engenders prominent radial features and a very thin outer ring along with highly nonequilibrium small fragments. The scale bar in both images corresponds to 50 μm.

prominent, whereas very slow evaporation decreases the importance of both azimuthal and radial instabilities, leading to a more uniform ring of deposits.

The width of the spaghetti threads increases toward the drop center, implying that the threads formed later are wider. This may be due to an increase in the polymer availability with time. The width and density of threadlike features are dependent on the rate of evaporation (volatility of solvent) and concentration of the polymer in the drop (which depends on solubility as well as the rate of dissolution vis-à-vis rate of evaporation). The width distribution of the polymer threads ("spaghetti" features) is shown in Figure 7 for the two different solvents evaporated under the ambient conditions where spaghetti features had a prominent appearance. The threads with 10−15 μm width have highest occurrence in both the cases, which may be due to compensatory effects of solubility and rate of evaporation. While toluene has lower solubility compared to that of ethyl acetate, its vapor pressure is also lower, resulting in a lower rate of evaporation. The lower solubility should engender thinner threads since less material is available, and the lower rate of evaporation should encourage a more uniform deposit consisting of fewer distinct threads of increased individual width. Indeed, decreasing the rate of evaporation by carrying out evaporation in a toluene vapor filled cell showed the change in patterns (Figure 8a) compared to Figure 5 for the ambient evaporation. Figure 8a shows a single, less undulating wide ring left behind by a drop evaporated nearer to the equilibrium conditions. The time required for complete drying in this case was 760 ± 20 s compared to 50 s for drying under ambient. The absence of distinct spaghetti features is quite noticeable. The wavelength of undulations along the ring is also much larger than that in Figure 5. The width of the ring is nearly uniform and is 30 ± 3 μm. Slower, near equilibrium rate of evaporation, resulting slower contact line movement, and weaker concentration and temperature gradients make all the

flows weak (less flow toward the periphery, more diffused convection cells of greater azimuthal width). These effects should engender more uniform polymer distribution, coupled possibly with a suppression of contact line instabilities and microscopic stick−slip, resulting in a more uniform ring stain. Also, the case of very slow evaporation on a dissolving substrate was, as expected, found similar to slow evaporation of a saturated polymer solution (results not shown). In such a case, competition between the rates of evaporation and substrate dissolution is lost, resulting in a high more uniform polymer concentration initially.

In contrast to the cases of slow evaporation (Figure 8a) and the medium rate of evaporation (Figure 5), increasing the rate of evaporation in a slow stream of dry nitrogen changes the polymer patterns as shown in Figure 8b. The time for complete evaporation of the drop was about 12 s, which is reduced by a factor of 4 compared to the medium rate of evaporation in the ambient. The highly nonequilibrium features in this case lack uniformity and parallel spaghetti features have a prominence of radial finger-type structures originating from a very thin outer ring. Secondary smaller fragments that are apparently randomly distributed indicate rather nonuniform fast contact-line activity in this far from the equilibrium case. Widely spaced multiple rings structures could be discerned on the droplet length scale (not shown) indicating macroscopic stick−slip. A lack of fine spaghetti threads in this case is indicative of fast drying of the thinner contact-zone regions, leading to a fragmented contact zone and the lack of repeated cycles of polymer buildup and deposition during the initial short time contact zone is more uniform.

The wavelength of undulations or the average spacing between the fingers consistently declines with increased rate of evaporation. For example, the measured wavelengths are 248, 121, and 105 μm for evaporation of in toluene vapors, ambient, and dry nitrogen, respectively. With increased evaporation, the Benard convection as well as the thermocapillary flow become stronger, which in turn should produce more concentration nonuniformity and stronger solutal-Marangoni and osmotic-pressure-driven flows as well. Among other things, increased rate of evaporation also decreases the average concentration of the polymer in the solution since less time is available for the substrate dissolution. This explains the smaller and narrower features. In addition, a lower viscosity dilute solution depins more readily[1] and should form more unstable contact lines, thus encouraging multiple rings and fragments in the case of high evaporation rate, as well as in the case of low solubility discussed later. First, it is instructive to examine and contrast the patterns formed on a nondissolving substrate from varying concentration of polymer solutions.

Figure 9 shows the result of features formed by evaporating drops of polymer solution dried on a *non-dissolving* glass substrate. Figure 9a shows the narrow multiple rings formed after drying of a low concentration 0.1 wt % solution, clearly indicating macroscopic stick−slip motion of a dilute solution directly observed in Figure 9b. These features are similar to the case of high evaporation. In contrast, Figure 9c shows much bigger, radially oriented fingers of higher interfinger distance formed by drying a solution of higher concentration (1 wt % polymer). This is similar to increased finger spacing at lower rate of evaporation, which should also lead to higher polymer concentration in the case of a dissolving substrate. At even higher concentrations, thick residual films were left, which exhibited cracks upon drying. However, the composite spaghetti features with fingers were never observed during the drying of a solution on glass. It should

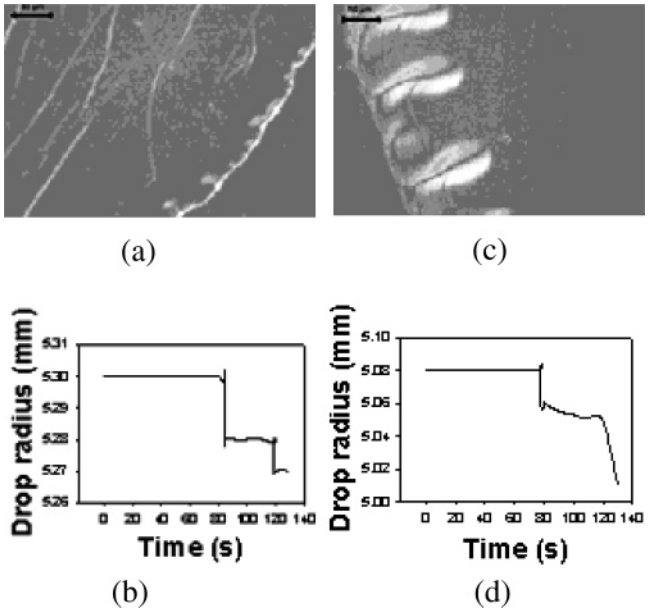

Figure 9. Polymer solution dried on a nondissolving glass substrate. (a) Pattern in a drop of 0.1 wt % PMMA solution. (b) Change in average drop radius with time for 0.1 wt % PMMA solution on glass. (c) Pattern in a drop of 1 wt % PMMA solution. (d) Change in average radius with time for 1 wt % PMMA solution on glass. The change in drop diameter indicates macroscopic stick−slip movement of the contact line. The scale bar in both the images corresponds to 50 μm.

also be noted that polymer solution at all concentrations showed initial pinning followed by a rapid slip (Figure 9d and multiple macroscopic stick−slip at small concentration; Figure 9c), which is in contrast to a continuous contact-line movement on dissolving substrates (Figure 3). There are couple of important lessons from the experiments on polymer solutions, in contrast to the results from a dissolving substrate. First, the parallel fine threadlike deposits (spaghetti features) form only in the absence of strong pinning of the contact line and, in particular, form only with its slow continuous movement. Therefore, explanation of spaghetti features in terms of multiple Benard cells (Figure 6b) in our system is less attractive, since all other conditions being same, these should form readily also in polymer solutions with strong pinning. A more likely scenario is thus a repeated cycle of solution supersaturation, deposition, and depletion near the slowly moving contact line on a dissolving substrate. Second, the rate of evaporation and the duration of initial contact line pinning (∼80 s) are similar at both the polymer concentrations, and yet, the spacing between the fingers is substantially increased at higher solution concentration. This implies an important role for the solutal Marangoni convection (Figure 6d), which should grow weaker at high bulk concentrations since surface gradients of polymer concentration in the contact zone should also become weaker as much of the surface there would experience a more uniform concentration. It may be reiterated that peripheral concentration is already substantially higher than the bulk because of the radially outward flows, and the surface concentration is expected to be even higher due to evaporation of solvent. A weaker and thus more diffused solutal Marangoni convection because of weaker surface tension gradients (Figure 6d), together with larger amount of polymer available, can thus explain more uniform deposits consisting of broader fingers with increased finger spacing and some filling of the interfinger spaces as well.

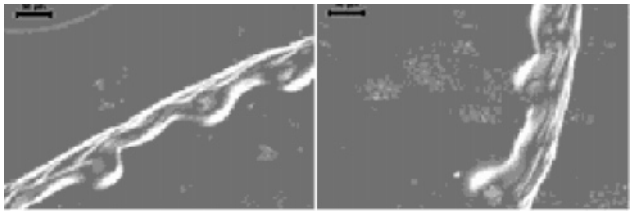

Figure 10. Pattern after evaporation of an ethyl acetate (higher solubility of PMMA) drop in the ambient. These images show the ring deposit is of a lesser width with far fewer striations. The scale bar corresponds to 50 μm.

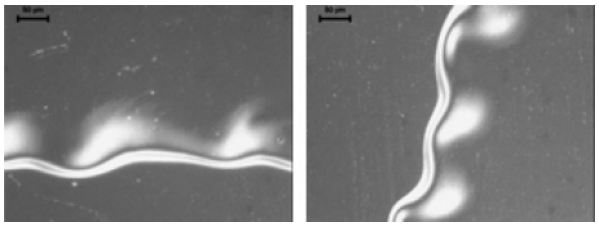

Figure 11. Pattern formed after evaporation of chloroform drop in the ambient (medium vapor pressure and medium solubility). The striation patterns are absent, and the frequency of undulation of the contact line is slightly higher than the case of ethyl acetate. The ring width is also smaller. The scale bar corresponds to 50 μm.

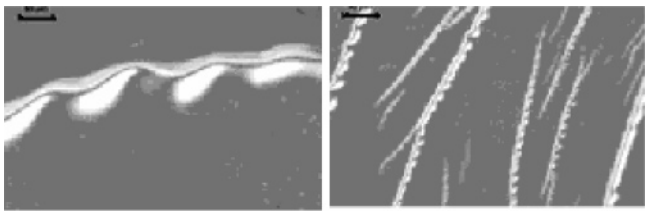

Figure 12. Pattern formed after evaporation of dichloromethane drop in the ambient (high vapor pressure and low solubility). The images show the absence of spaghetti features, the ring width is much smaller, and multiple rings indicative of macroscopic stick slip are formed. The undulation frequency of the contact line is also larger. The scale bar corresponds to 50 μm.

The effect of solvent or polymer solubility can also be examined in view of the above and the earlier discussion related to the effect of rate of evaporation. The average width of ring deposit in the case of highest solubility and the lowest vapor pressure solvent used, ethyl acetate, is about 64 μm (Figure 10), which declines to 32.4 μm (Figure 11) for chloroform, which is a medium solubility and medium vapor pressure solvent. Further, the lowest solubility and highest vapor pressure solvent used (dichloromethane) exhibits a ring width of 26.7 μm. This indicates that the total dissolved polymer available in the drop during its evaporation was less for poorer solvents and higher rates of evaporation. All the measurements of ring width were averaged over a minimum of 10 locations along the circumference of the ring.

As discussed earlier, increased rate of evaporation also engenders decreased finger spacing by stronger thermal and solutal convections. This is also supported by the data on different solvents (Figures 10−12). The wavelength of undulations is 198, 150, and 113 μm for increasing vapor pressure solvents, ethyl acetate, chloroform, and dichloromethane, respectively. In addition, patterns in the higher volatility solvents (Figures 11 and 12) even show undulations of the outer edge of the ring deposit. For the highest volatility (Figure 12), the formation of multiple rings is also seen which is not noticed in the other cases.

Ellipsometric measurements showed that thickness of the PMMA substrate underneath the drop decreased almost uniformly by about 30 nm after complete evaporation of a 3 mm diameter toluene drop in the ambient. Since the initial PMMA layer thickness was 200 nm, a reservoir of polymer was available in all of the above experiments. The effect of polymer depletion was studied by toluene evaporation on a much thinner 20 nm thick PMMA film. Ellipsometric measurements indicated that the entire PMMA layer was dissolved from underneath the drop and redeposited near the periphery. The patterns formed in this case (Figure 13) lack the spaghetti features, as well as the structural complexity and variety seen on a 200 nm thick PMMA layer (Figure 5). Only the finger-type structures forming out of a thin outer ring are seen. The shape, size, and the spacing of fingers in this case were much more uniform along the entire periphery compared to the structures in Figure 5. The wavelength of these undulating structures was 71 μm, as compared to 120 μm on a 200 nm thick substrate under identical conditions. This is similar to decreased finger spacing with decreased polymer concentration (Figure 9). No multiple rings were witnessed due to a complete depletion of polymer after the development of initial features.

Conclusions

The simple process of evaporation of solvent drops on dissolving polymer substrates yield complex "coffee-stain" surface patterns near the initial drop periphery. The most complex pattern consists of rather regular variations of deposit thickness both in the radial direction (formation of parallel "spaghetti" threads) and along the periphery (formation of radially oriented hills or fingers). The pattern morphology is dependent on the rate of evaporation, solubility of the polymeric substrate, and also on the thickness of the dissolving substrate if it is small. The formation of successive spaghetti threads without the occurrence of macroscopic stick−slip indicates an alternate mechanism to repeated macroscopic pinning and depinning events of the contact line. The closely spaced polymer

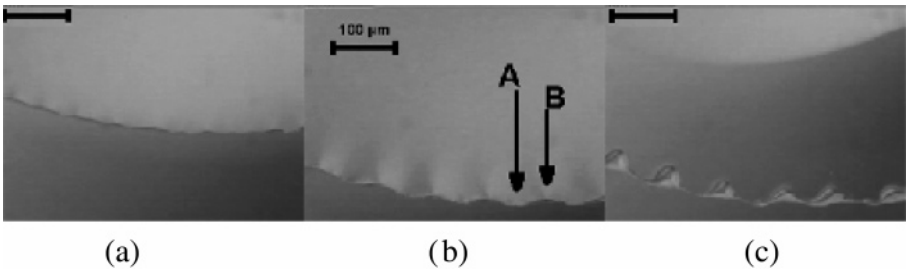

Figure 13. Development of spatially periodic flows in the contact zone during evaporation of a toluene drop in ambient on a 20 nm thick PMMA film. The images are at various time intervals: (a) 5, (b) 12, and (c) 20 s. Flow along the contact line could be discerned from thinner regions A to thicker regions B, where polymer deposition in the form of fingers finally occurs. The scale bar corresponds to 100 μm. Finger structures are seen in this case on complete evaporation (c).

threads occur only at intermediate rates of evaporation and with enough polymer available for dissolution. Increased rate of evaporation leads to the formation of more prominent fingerlike structures by a rapid fragmentation of the contact zone along the drop periphery and the occurrence of multiple widely separated rings plus random fragments by macroscopic stick slip motion of the contact line. The slow rate of evaporation leads to weaker flows and near equilibrium deposits consisting of a single ring of uniform width and height.

These observations point to new possibilities for the control and formation of finer and densely packed structures by modulating the rate of evaporation, solubility, and film thickness. We also have discussed several mechanisms and their synergies responsible for a nonuniform deposition of polymer along a contact line. There is however no existing theory to quantify the net effect of these flows on the polymer pattern selection. It is hoped that this study will also motivate a better understanding of the flow mechanisms and provide a rational tool for the creation of more controlled patterns.

Acknowledgment. The help received from Joydeep Guha in the early phases of this study is gratefully acknowledged. This study was supported by the Department of Science and Technology, India, through its Nanoscience Program.

LA0362268